

Conformational Stability and Spin States of Cobalt(II) Acetylacetonate: CASPT2 and DFT Study

Mariusz Radoń,^{*,†} Monika Srebro,[†] and Ewa Broclawik[‡]

Department of Theoretical Chemistry, Jagiellonian University, ul. Ingardena 3, 30-060 Kraków, Poland, and Institute of Catalysis and Surface Chemistry, Polish Academy of Sciences, ul. Niezapominajek 8, 30-239 Kraków, Poland

Received December 22, 2008

Abstract: Electronic structure and conformation of bis(acetylacetonate) cobalt(II), $\text{Co}(\text{acac})_2$, a prototypical mediator in controlled radical polymerization of olefins, is reinvestigated. The ab initio multiconfigurational CASSCF/CASPT2 method is used to resolve the doubts stemming from density functional theory results. We assign the quartet ground state for a single molecule and point at tetrahedral conformation as the preferred one. Several density functionals are tested against the ab initio calculations, and their performance is assessed. The strength of intermolecular interactions in the crystal structure composed of square-planar $\text{Co}(\text{acac})_2$ molecules (Burgess, J.; et al. *Acta Crystallogr.* 2000, C56, 649–650) is estimated to be sufficient for their planarization (suggested by Matyjaszewski, K.; et al. *Chem.–Eur. J.* 2007, 13, 2480–2492).

1. Introduction

Bis(acetylacetonate) cobalt(II), $\text{Co}(\text{acac})_2$, and its derivatives were recently proposed as mediators in controlled radical polymerization (CRP) of olefins. Cobalt-mediated CRP is based on the propensity of four-coordinated cobalt(II) complexes to reversibly capture organic radicals, thereby buffering their concentration at the desired level.¹ In theoretical studies on such reactions, the issues of great importance are to identify the spin symmetry and the lowest-energy conformation of the cobalt moiety and to investigate how these properties are affected by a coordination of an extra ligand (an organic radical). However, despite several studies treating $\text{Co}(\text{acac})_2$, the issues of spin state and preferred conformation of this deceptively simple compound are not yet definitely closed.^{2–7}

Two conformations were proposed for the $\text{Co}(\text{acac})_2$ molecule: tetrahedral (of D_{2d} symmetry) and square-planar (of D_{2h} symmetry)^{2–5} (Figure 1). According to the experiments from the 1960s, the $\text{Co}(\text{acac})_2$ monomer was claimed to be tetrahedral,³ which was also supported by a crystal structure resolution.⁴ However, this crystal structure consists

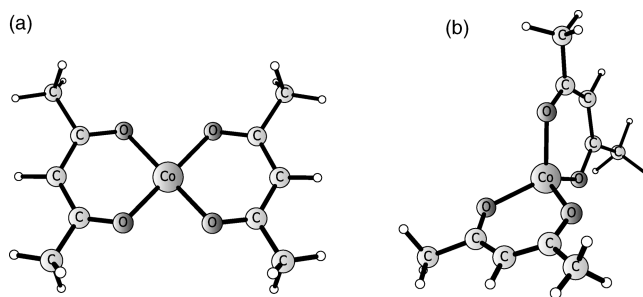


Figure 1. Alternative conformations for $\text{Co}(\text{acac})_2$: (a) square-planar and (b) tetrahedral.

not of isolated molecules but of tetramers, where $\text{Co}(\text{acac})_2$ units are chemically bound (share oxygens) and the coordination is effectively octahedral; therefore, this structure is not necessarily related to the isolated molecule. Quite surprisingly, a more recent (from 2000) crystal structure is built of square-planar $\text{Co}(\text{acac})_2$ molecules, while no significant intermolecular interactions were claimed.⁵ This recalled the original notion of square-planar conformation² (undermined in ref 3). The existence of stacking interaction between parallel arranged monomers in the crystal structure from ref 5 was suggested to affect the preferred conformation,⁶ though the strength of these forces was not assessed at a quantitative level.

* Corresponding author e-mail: mradoń@chemia.uj.edu.pl.

[†] Jagiellonian University.

[‡] Polish Academy of Sciences.

In addition to two alternative conformations, two different spin states are possible for seven 3d electrons of cobalt(II): doublet (low-spin) and quartet (high-spin). No definite experimental evidence for any of them has been presented in the literature; nevertheless, the magnetic moment measurements from the 1960s opt for a high-spin ground state.² We note that some experiments on $\text{Co}(\text{acac})_2$ are difficult to interpret or even inconclusive in terms of its electronic structure. For instance, the toluene solution of $\text{Co}(\text{acac})_2$ has been described as EPR silent,^{6,8} which is contradictory to a paramagnetic nature of both spin states, and caused presumably by a fast spin relaxation.

Recent density functional theory (DFT) calculations on $\text{Co}(\text{acac})_2$ actually predicted the high-spin ground state in tetrahedral conformation,^{6,9,10} yet these studies were based solely on the hybrid (B3LYP, B3PW91*) functionals, which are known to (sometimes erroneously) favor the high-spin states.¹¹ We shall demonstrate here that with a different choice of density functional quite opposite results can be found, what questions the DFT quality for the present problem and calls for ab initio calculations to resolve the doubts.

In this study, complete active space self-consistent field/second-order perturbation theory (CASSCF/CASPT2)^{12,13} calculations are performed to unambiguously identify the ground state. This method is able to properly treat both exchange effects and strong (nondynamical) correlation present in transition-metal compounds,¹⁴ what was proven in several successful applications, notably in two recent works for a variety of iron(II) complexes.^{15,16} In the present study, CASPT2 energetics is contrasted with a DFT one and conclusions about the performance of various functionals are drawn.

As will be shown, high level ab initio calculations indicate a tetrahedral ground-state conformation, with strong support for the high-spin state. To shed more light on the reported crystal structural build of monomeric, square-planar $\text{Co}(\text{acac})_2$ units,⁵ thus at first sight contradicting our results, we also focus on prospective intermolecular interactions presumably causing a stacking arrangement.⁶ To this end, we estimate intermolecular interaction energy in a dimer of two planar molecules (roughly modeling the crystal), to judge whether this interaction is sufficiently strong to impose the planarity of the $\text{Co}(\text{acac})_2$ unit.

2. Methods and Models

The orientation of the $\text{Co}(\text{acac})_2$ molecule used in this study is given in Figure 2, where also the twist angle θ between the acac rings is defined (acac = acetylacetonate).

The symmetry was employed in all calculations: D_{2h} for square-planar conformation, D_{2d} for tetrahedral conformation, and D_2 for a general (twisted) form. The symmetry labels of orbitals and electronic states are given below in D_2 , as the highest common subgroup of all three groups.

For each conformation and electronic state, we performed (unrestricted) DFT geometry optimization (followed by frequency calculation and stability analysis). Turbomole¹⁷ and Gaussian 03¹⁸ packages were employed. In DFT

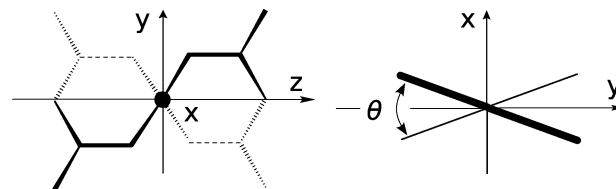


Figure 2. Orientation of $\text{Co}(\text{acac})_2$ molecule used in this study: top view (left) and side view (right). The twist angle (θ) is defined as the dihedral angle between the acac rings: zero for the square-planar, 90° for the tetrahedral, and $0 < \theta < 90^\circ$ for a general (twisted) conformation.

Table 1. Definitions of the ANO Basis Sets Used in This Study

basis set	definition
ANO1	Co: ANO-RCC 7s6p5d2f1g, ligands: ANO-S [O: 4s3p1d, C: 3s3p1d, H: 2s]
ANO2	ANO-RCC [Co: 7s6p5d3f2g1h, O: 4s3p2d1f, C: 4s3p1d, H: 3s1p]
ANO3	ANO-RCC [Co: 8s7p6d4f3g2h, O: 5s4p3d2f1g, C: 4s3p2d1f, H: 3s1p]

calculations, two types of basis set were tested: the smaller one (basis A) consists of ecp-10-mdf 6s5p3d1f (with pseudo-potential)¹⁹ on Co and 6-31G(d)^{20,21} on ligands; the larger one (basis B) consists of QZVPP²² on Co and TZVPP²³ on ligands. Various density functionals were applied, including (1) generalized gradient approximations (GGA): BP86,^{24,25} PBE,²⁶ OLYP,^{27,28} (2) meta-GGA: TPSS,²⁹ (3) hybrid GGA: PBE0,³⁰ B3LYP,³¹ and (4) hybrid meta-GGA: TPSSH.³² The influence of solvent on relative energies was estimated using conductor-like screening model (COSMO)³³ as implemented in Turbomole. The dielectric constant (ϵ) of 5.0 was chosen to mimic nonpolar solvents typical to CRP reactions. Apart from that, the infinite ϵ was tested as an upper estimation of nonspecific solvent effects.

CASSCF/CASPT2 energy calculations were performed with the Molcas 6.4 package^{34,35} for PBE0 (basis A) structures. The zero-order Hamiltonian for CASPT2 was the default one in Molcas (IPEA shift of 0.25 au³⁶) with extra imaginary level shift (0.1 au). Core orbitals were frozen in CASPT2 except 3s and 3p of Co, which were correlated. Three atomic natural orbitals (ANO) basis sets^{37,38} of increasing quality, denoted ANO 1–3, were used in the calculations (Table 1). Note that similar basis sets have been successfully employed in CASPT2 calculations for iron complexes.^{15,16} Scalar relativistic effects were included in the calculations via second-order Douglas–Kroll–Hess transformation.³⁹

The active space was composed of bonding and antibonding orbitals directly participating in the metal–ligand bond, the remaining Co 3d orbitals, and correlating Co 4d (double shell) orbitals. This choice covers the important nondynamical correlation effects in both the cobalt–ligand bond and the cobalt ion itself.¹⁴ It gives in total nine electrons in 11 orbitals (9 in 11) for the planar geometry and 11 electrons in 12 orbitals (11 in 12) for the tetrahedral geometry. The difference is situated in a different number of bonding–antibonding orbital pairs describing the metal–ligand bond: only one such pair exists for the square-planar conformation but

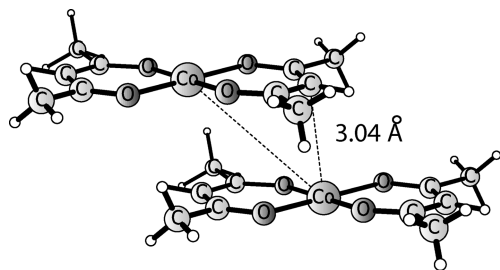


Figure 3. Dimer model, $[\text{Co}(\text{acac})_2]_2$.

two (symmetry equivalent) can be found for the tetrahedral form (see contour plots in the Supporting Information). In other words: for the tetrahedral form both Co $3d_{xz}$ and $3d_{yz}$ orbitals efficiently mix with the ligand orbitals, but for the square-planar form only $3d_{yz}$ does so, while the $3d_{xz}$ orbital interacts with the ligand orbitals very weakly, yielding the antibonding combination being almost pure metal orbital and the bonding combination being almost pure ligand orbital (Supporting Information). The latter ligand orbital (with a trace of $3d_{xz}$) was added to the (9 in 11) active space, to obtain the (11 in 12) active space, which is fully compatible with the (11 in 12) active space for the tetrahedral conformation. Nevertheless, it follows that both (11 in 12) and (9 in 11) active spaces lead to almost the same energies for the square-planar conformation (the difference being 0.1–0.8 kcal/mol, below a chemical accuracy). Thus, we conclude that the orbital added in (11 in 12) is indeed not important for the present problem. For these reasons, we recommend using the (9 in 11) active space for the square-planar form, as more intuitive and chemically motivated.

To probe intermolecular interactions in the crystal structure from ref 5, a dimer model was used (Figure 3). The coordinates were taken from the crystal structure and optimized at the PBE0 (basis A) level, constraining the C_{2h} symmetry. The Co–Co' and Co–C' distances (between the atoms of the neighboring molecules), which are the structural parameters most important for the stacking interaction, were frozen (in Figure 3 the frozen distances are indicated as dashed lines). The stabilization energies, with single point correction for basis set superposition error (BSSE),⁴⁰ are given with respect to isolated monomers in their optimal PBE0/A geometries. Unfortunately, the dimer model is already too large for CASPT2 calculations with the analogous active space as for the monomer. Therefore, the stabilization energies were obtained from Moeller–Plesset second-order perturbation theory (MP2) and approximated second-order coupled clusters model (CC2),⁴¹ both within the RI approximation, as well as from the selected DFT functionals. These calculations employed basis set B. All calculations for the dimer model were performed with the Turbomole package.

For further confirmation of the results from the dimer model, we also carried out analogous RI-MP2/B calculations for the trimer, which is a more realistic model of the crystal structure. For simplicity, the BSSE correction of –2.3 kcal/mol/single molecule was not computed for the trimer, but taken from the dimer calculations (this detail should not be crucial).

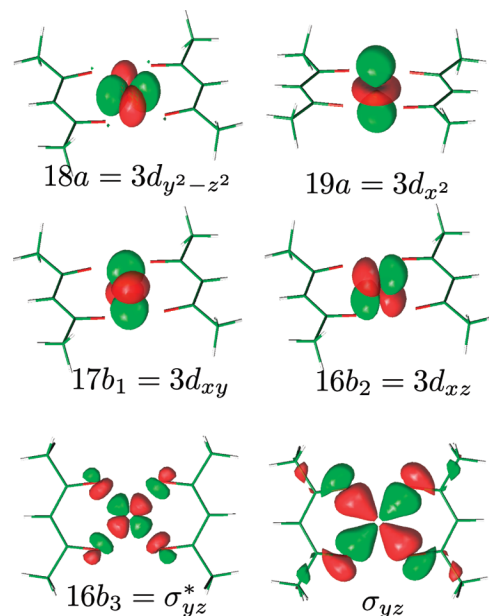


Figure 4. Selected active orbitals (9 in 11) for the square-planar conformation (0.04 $\text{au}^{-3/2}$ isovalue).

3. Results and Discussion

3.1. Electronic Configurations and Structures. In the coordination environments of both square-planar and tetrahedral conformations, three of five Co 3d orbitals remain almost pure metal orbital (i.e., do not mix significantly with any ligand orbitals): $3d_{z^2}$ and $3d_{x^2-y^2}$ (18,19a), and $3d_{xy}$ (17b₁). The situation of the remaining two Co 3d orbitals depends on the conformation. For the tetrahedral geometry, both $3d_{xz}$ and $3d_{yz}$ orbitals are destabilized by significant interactions with the corresponding ligand orbitals, yielding $16b_2 = \sigma_{xz}^*$ and $16b_3 = \sigma_{yz}^*$ antibonding orbitals (and their bonding counterparts: σ_{xz} , σ_{yz}). For the square-planar geometry, only $3d_{yz}$ is involved in the similar interaction with a single ligand orbital, yielding $16b_3 = \sigma_{yz}^*$ (and its bonding counterpart: σ_{yz}), while $3d_{xz}$ remains almost pure metal orbital. The contour plots of the discussed orbitals are given in Figures 4 and 5 (the figures show the CASSCF natural orbitals, but DFT orbitals are qualitatively similar).

Now it is useful to take a look at the low-lying electronic states considered in this study (candidates for the ground state, or at least the lowest state for each conformation) and analyze their dominant configurations. For the tetrahedral structure, the lowest quartet state is (regardless the method) $^4A = (18a)^2(19a)^2(17b_1)^1(16b_2)^1(16b_3)^1$ (having unpaired electrons in $3d_{xy}$, σ_{xz}^* , and σ_{yz}^*). For the square-planar conformation, either $^2A = (18a)^2(19a)^1(17b_1)^2(16b_2)^2(16b_3)^0$ (having an unpaired electron in $3d_{x^2}$) or $^2B_2 = (18a)^2(19a)^2(17b_1)^2(16b_2)^1(16b_3)^0$ (having an unpaired electron in $3d_{xz}$) is the lowest doublet state (depending on the method); therefore, both 2A and 2B_2 will be considered below. As also found in the other study,⁶ the tetrahedral geometry does not yield a stable minimum in the doublet state, the geometry always converging to the planar minimum. In other words, the tetrahedral doublets are unstable with respect to twisting of the acac rings (the θ angle, Figure 2), converting one conformation into another. The lowest quartet state for the square-planar conformation is (for all methods) $^4B_1 =$

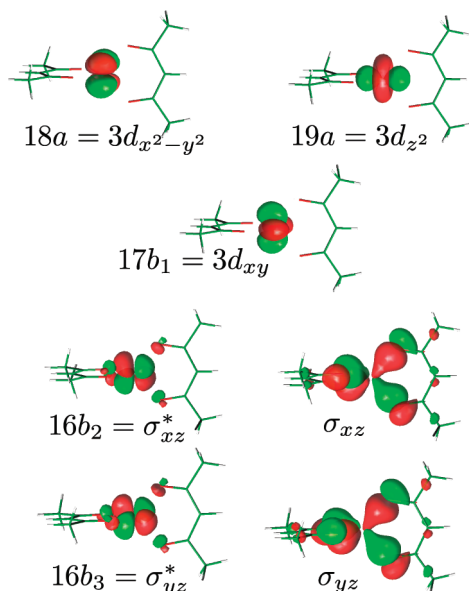


Figure 5. Selected active orbitals (11 in 12) for the tetrahedral conformation (0.04 au^{-3/2} isovalue).

Table 2. Cobalt–Oxygen Distance (in Angstroms)

DFT, $S = 1/2$	1.85–1.90 ^a
DFT, $S = 3/2$	1.94–2.00 ^a
expt, tetrahedral (tetrameric) ⁴	1.93–2.13 ^b
expt, square-planar ⁵	1.92

^a Depending on the functional. ^b Nonequivalent bond lengths found in the crystal.

(18a)¹(19a)²(17b₁)²(16b₂)¹(16b₃)¹, having unpaired electrons in 3d_{y²-z²}, 3d_{xz}, and σ_{yz}^* . This state is also unstable with respect to θ -twisting mode, in agreement with ref 6. However, it was found that another quartet state (of only slightly higher energy) gives a stable minimum for the planar conformation: ⁴B₃ = (18a)¹(19a)¹(17b₁)²(16b₂)²(16b₃)¹, having unpaired electrons in 3d_{y²-z²}, 3d_{x²}, and σ_{yz}^* . Thus, both ⁴B₁ and ⁴B₃ square-planar quartets will be considered.

All tested DFT methods yield very similar geometries for the respective electronic states. (It is generally recognized that different density functionals usually predict very similar structures,^{42,43} which is certainly not the case for spin-state energetics.) The representative PBE0/A structures (i.e., those used in CASSCF/CASPT2) can be found in the Supporting Information. Herein we discuss only the key structural parameter, which is the cobalt–oxygen distance (Table 2, DFT values from different functionals are given as ranges for simplicity). The cobalt–oxygen distance, depending mostly on the spin state, is significantly longer in the high-spin than in the low-spin states. This trend is understandable since antibonding metal–ligand orbitals (σ_{yz}^* , σ_{xz}^*) are occupied in the quartets, but not in the doublets. In a complementary view, the ionic radius of a cobalt cation increases with the increase of spin multiplicity, so the 3d unpaired electrons can better avoid each other in space. The computed Co–O distance for the quartets is close to the bond length characteristic for the oligomeric tetrahedral structure. The experimental value for the other crystallographic structure (with square-planar molecules) is shorter, which would suggest the doublet state. However, this distance falls

Table 3. Energies (kcal/mol) of the Square-Planar Doublets and Quartets with Respect to the Tetrahedral ⁴A

	$S = 1/2$		$S = 3/2$	
	² A	² B ₂	⁴ B ₁	⁴ B ₃
DFT/Basis A				
PBE0	17.4	20.2	8.6	11.6
B3LYP	12.1	14.4	8.6	12.1
BP86	3.5	1.1	9.3	12.7
PBE	3.8	0.8	8.9	12.5
OLYP	8.5	7.2	8.8	11.4
DFT/Basis B				
PBE0	13.5	15.7	9.8	12.0
B3LYP	9.8	11.0	9.4	12.0
BP86	−0.5	−3.7	10.7	13.7
PBE	−0.5	−3.9	10.3	13.4
OLYP	5.5	4.0	10.0	12.6
TPSS	0.9	−0.9	11.7	14.7
TPSSH	6.9	7.5	11.1	14.2
CASPT2/ANO 1–3				
ANO 1	18.2	15.0	9.9	11.2
ANO 2	16.6	13.2	9.0	10.3
ANO 3	16.7	13.2	9.2	10.4

between the calculated ones for the doublet and the quartet electronic states. For the present case, it is therefore impossible to assign the spin state solely on the basis of the cobalt–oxygen bond length. The analysis of relative energies in the next section attempts to fill this gap.

3.2. Relative Energies: CASPT2 vs DFT. DFT and CASPT2 energies of the square-planar doublet (²A, ²B₂) and quartet (⁴B₁, ⁴B₃) states relative to the tetrahedral quartet (⁴A) state are given in Table 3.

First of all, rather strong dependence of DFT results on the basis set can be observed in agreement with some previous studies.^{16,44} Unless otherwise stated, we refer to the results from the larger basis. It can be seen that hybrid density functionals (B3LYP, PBE0) predict a tetrahedral quartet (⁴A) ground state, being separated from the square-planar doublets and quartets by a clear gap of at least 10 kcal/mol. On the other hand, classical GGA functionals (BP86, PBE) yield a completely different picture with the lowest doublet and quartet close in energy (separated by ~4 kcal/mol or less). In the larger basis set, the planar doublet eventually becomes the ground state. Meta-GGA functional (TPSS) behaves very similarly to GGA in this respect. Interestingly, somewhere between these extremes there are two other functionals: OLYP (a GGA based on the OPTX exchange²⁷) and TPSSH (hybrid meta-GGA, containing only 10% of Hartree–Fock exchange). It is clear that the doublet–quartet splitting in Co(acac)₂ strongly depends on the applied functional, particularly on the admixture of Hartree–Fock exchange in the exchange potential. A qualitatively similar trend was observed in several DFT studies (see refs 15 and 45 and references therein). It is worth noting here that the (adiabatic) DFT doublet–quartet splitting for Co(acac)₂ ranges from −3.9 (PBE) to 13.5 (PBE0). This uncertainty is a warning that DFT calculations cannot be safely used to determine the ground-state multiplicity of Co(acac)₂.

The CASPT2 calculations predict the high-spin ⁴A (in the tetrahedral conformation) to be the ground state. The lowest doublet (²B₂) lies about 13 kcal/mol above; the lowest square-

Table 4. Doublet–Quartet Splitting in Free Co(II) Ion

		ΔE (² G– ⁴ F) (cm ^{−1})	error (kcal/mol)
6s5p4d2f1g		16651	0.4
7s6p5d2f1g	(ANO 1)	16488	−0.1
7s6p5d3f2g1h	(ANO 2)	16258	−0.7
8s7p6d4f3g2h	(ANO 3)	16140	−1.1
exptl ^a	(NIST ⁴⁷)	16510	0

^a Average energy of spin–orbit terms.

planar quartet (⁴B₁) lies about 9 kcal/mol. These results are stable as the basis set is increased: going from ANO 2 to ANO 3 has only a minor impact on the relative energies, and therefore the results seem to be converged with respect to basis set. To further analyze the basis set dependence, we investigated doublet–quartet (²G–⁴F) splitting in the free cobalt(II) ion, a property that is known experimentally with high accuracy. As argued elsewhere, the basis set error on the Co(acac)₂ doublet–quartet splitting can be partially traced back to the analogous error on the atomic excitation energy.^{15,46} The experimental data was obtained from the National Institute of Science and Technology (NIST) Atomic Spectra Database⁴⁷ by averaging the energies of spin–orbit terms according to the procedure described elsewhere.⁴⁶ The theoretical CASPT2 results were computed with 3d4d active space for various contractions of the ANO-RCC basis set, corresponding to ANO 1–3 (Table 4). It follows that for free Co(II) ion CASPT2 is accurate up to ~1 kcal/mol for all the tested basis sets, even the smallest one. (It might be interesting that starting from ANO 1 the error slightly increases as basis set is increased; obviously, this behavior is rooted in an approximate character of the CASSCF/CASPT2 method itself.) The error falls within chemical accuracy and is fully acceptable for all cases. Interestingly, in this atomic calculations the CASPT2 method tends to slightly favor the low-spin state; it does not reveal any tendency to overstabilize the high-spin state. This observation supports the previous conclusion about the quartet ground state.

CASPT2 state ordering can be satisfactorily reproduced only by hybrid functionals (B3LYP, PBE0). Nonhybrid functionals (maybe except OLYP) artificially favor the low-spin states and thus yield different (and probably wrong) results. On the other hand, all tested functionals accurately reproduce the energy difference between the planar and the tetrahedral conformations for the high-spin states. While DFT apparently has problems with spin-state energetics, these problems do not affect the energy of a simple conformational transition not accompanied by a spin flipping.

Thus far, only electronic energy differences were discussed. Two other factors that might discriminate between alternative electronic states are vibrational energies and solvent effects. Their impact on relative energies is described in the Supporting Information. Here, we summarize that the addition of zero-point vibrational energies further increases (by ~1 kcal/mol) the relative energies of the square-planar doublets, while it has much smaller influence on the relative energies of the square-planar quartets (with respect to the tetrahedral quartet). Thus, considering vibrational energies by no means alters our previous conclusion about the ground state; conversely: the high-spin ground state is stabilized even

Table 5. Stabilization Energy (kcal/mol) per Single Co(acac)₂ Molecule Estimated from the Dimer Model

	doublet	quartet
RI-MP2	9.5	9.5
RI-CC2	11.1	10.2
HF	1.2	2.2
PBE0	2.9	3.0
PBE	2.4	3.7
BP86	0.8	−0.4

more. On the other hand, the polarizable continuum stabilizes the square-planar conformation by 1–2 kcal/mol with respect to the tetrahedral one. This influence is definitely too small to change the ground-state identity. Therefore, we do expect the same ground state in vacuum as in an apolar, noncoordinating solvent.

3.3. Stacking Energy in the Crystal Structure. According to the above CASPT2 calculations, the high-spin state in tetrahedral conformation should be preferred by at least 10 kcal/mol. Nevertheless, the recently published crystal structure consisting of square-planar molecules⁵ appears to contradict this result, which calls for explanation. To this end, we focused on prospective intermolecular interactions favoring the planar conformation. Indeed, it was pointed out that in the crystal structure the molecules are loosely stacked on top of each other,⁶ and thus the resulting stacking interactions (weak “sandwich” coordination of cobalt by π electrons of the neighboring acac ring and/or dispersion) might stabilize the planar form, explaining its presence in the crystal. However, if it were the correct explanation, the stabilization should be stronger than 10 kcal/mol/single molecule (the amount of energy by which the tetrahedral conformation is preferred in vacuum), which seems quite large. Please note that the distance from Co to the nearest neighbor acac ring is ~3 Å (cf. Figure 3 and ref 5). Therefore, we attempted to assess the strength of the stacking interaction at a quantitative level.

To this end, we used the dimer model representing the considered crystal structure (details in section 2). The interaction energies were computed with respect to the doublet (²A) and quartet (⁴B₁) states of monomers. Thereby, two spin states were considered for the dimer: the triplet (i.e., the dimer of doublets) and the septet (i.e., the dimer of quartets). As expected, the stabilization energies were very similar for both spin states. The computed stabilization energies per single molecule are given in Table 5 (note that a positive sign of stabilization energy indicates stabilization, and negative indicates destabilization).

Single reference ab initio methods (MP2, CC2) yield a very similar and quite large dimer stabilization energy, on the order of 20 kcal/mol, i.e., 10 kcal/mol for a monomer. It is larger than one would expect for “typical” intermolecular interactions. The known cobalt complexes where some ligands are loosely bound to Co via delocalized π electrons¹⁰ should be recalled here. Likewise, the delocalized π density of the acac ligand can coordinate the cobalt ion from the neighboring molecule. Let us note, however, that the intermolecular distance is large (~3 Å). Therefore, we do not attempt to firmly quantify the role of chemical interaction or just dispersion forces in the net stabilization energy. A

more systematic treatment, such as symmetry-adapted perturbation theory,⁴⁸ would be desirable for this purpose, but such a study is beyond the scope of the present investigation. Let us note, however, that HF and the tested DFT methods predict only very small stabilization and — as these methods do not account properly for dispersion effects, while MP2 and CC2 do — this could indicate a dispersion as an important ingredient of stabilization. We do not rule out, however, the possibility of a weak chemical bond with π electrons of the acac ring. Given the poor performance of the tested DFT methods for the stabilization energy (Table 5), we suspect that recently developed hybrid meta-GGA functionals, demonstrated to better reproduce stacking energies in organic systems,⁴⁹ might be somewhat better suited for this task.

By definition, the stacking interaction discussed above affects only the planar conformation. Certainly, some intermolecular interaction would also affect the tetrahedral conformation, but this interaction should presumably be much smaller. Roughly speaking, it is the planarity of the $\text{Co}(\text{acac})_2$ molecule that warrants its strong, favorable interaction with the other (also planar) molecule. We believe therefore that the rigorous assessment of weak intermolecular interactions affecting the tetrahedral structure (a very demanding project, including the search for the most favorable crystal structure with tetrahedral cobalt) is not obligatory here. Thus, the stabilization gained by the square-planar conformation due to stacking interaction could indeed compensate for its intrinsically higher energy, which could explain (at a semiquantitative level) the apparent discrepancy between theoretical geometry of a monomer and the crystallographic structure from ref 5. Nevertheless, higher-order ab initio calculations of stabilization energies, for instance with CCSD or CCSD(T), would be desirable for further confirmation. These calculations are beyond our computational power, though.

It is worth noting here that the actual stabilization energies (in the frame of MP2 and CC2 methods) could be even higher than those computed here. First, this could be because of the applied correction for basis set superposition error, which is often claimed to make binding energies too low. Second, the dimer model is likely to give a too-small stabilization energy compared to that of the crystal lattice (assuming full additivity of the nearest neighbor interactions, the dimer model would give only a half of the actual stabilization energy). However, the main drawback of the dimer model is that the $\text{Co}(\text{acac})_2$ unit has only one neighbor (from one side), while in solid it has two neighbors (from both sides). In this respect, the trimer model would be a much better approximation. We have therefore performed RI-MP2 calculations for the trimer model, which gave a stabilization energy of 13.5 kcal/mol per single molecule, even larger than that for the dimer model, which supports our conclusions.

Let us now hypothesize on the spin state of $\text{Co}(\text{acac})_2$ present in the lattice reported in ref 5. According to the above CASPT2 results (cf. Table 3), the quartet ($^4\text{B}_1$) is the lowest spin state for the square-planar conformation, the lowest doublet state lying ~ 4 kcal/mol above. We also saw that the stacking interaction does not discriminate between

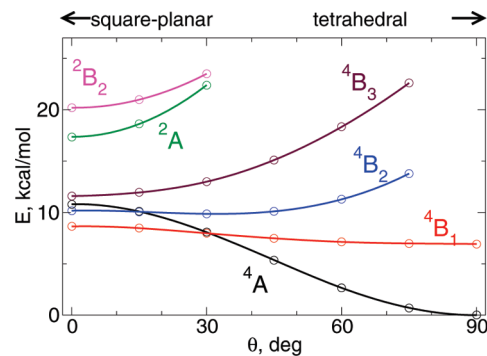


Figure 6. Electronic energy curves (PBE0, basis A) as a function of the twist angle θ . The $^4\text{B}_1$ and $^4\text{B}_2$ states are (negligibly) unstable at $\theta = 0$, having instead shallow minima at $\theta = 90^\circ$ and $\theta \approx 30^\circ$, respectively.

doublet and quartet states of monomers (cf. Table 5). Therefore, most probably the high-spin state is “frozen” inside the crystal. This prediction seems also supported by a low-temperature, solid-state EPR spectrum registered by Sojka et al.⁷ The suspected presence of a square-planar quartet state in the crystal cannot be diminished by its conformational instability reported in section 3.1. First, the other quartet state $^4\text{B}_3$, being perfectly stable at square-planar geometry, lies only ~ 1 kcal/mol above $^4\text{B}_1$. Such closely lying states could be, in fact, strongly coupled via a spin–orbit term (not accounted for here), losing their exact orbital symmetry. Second, the instability for $^4\text{B}_1$ is actually very weak. To check its importance, we computed potential energy curves (in a function of θ) for $^4\text{B}_1$ and the other relevant states (Figure 6). Evidently, the energy curve for $^4\text{B}_1$ is almost flat, indicating only a negligible instability, which could be easily hindered in a solid, particularly here, in the presence of strong π -stacking interactions.

4. Conclusions

The ground state of bis(acetylacetonate) cobalt(II) was identified as high-spin and tetrahedral by means of ab initio CASPT2 calculations with a high credibility level. In variance, DFT results for $\text{Co}(\text{acac})_2$ substantially depend on the exchange functional. The comparison with CASPT2 supports the results from the hybrid functionals with 20–25% of HF exchange (B3LYP, PBE0). Nonhybrid ones (BP86, PBE, OLYP, TPSS) overstabilize the low-spin state and are in disagreement with CASPT2 by 9–10 kcal/mol or more, in some cases (BP86, PBE) predicting even the wrong spin state and the wrong conformation. Also, the OLYP functional, supported by several successful comparisons with experiment or ab initio calculations,^{16,50,51} is herein quite far from CASPT2 (though not as far as classical GGA: BP86 and PBE).

The conclusions about DFT performance, drawn here by comparison with CASPT2, have a benchmark value and can be used to choose the optimal functional for similar compounds (e.g., with substituted acac ligands). The wise choice of density functional is particularly important for modeling CRP and other reactions involving $\text{Co}(\text{acac})_2$ or derivatives. In the studies on reaction mechanisms, the big size and low symmetry of the models and other technical

difficulties usually make ab initio calculations prohibitively expensive, thus nolens volens one must stick to DFT. Thus, given the CASPT2 results, we recommend the hybrid functionals for the present and similar cases. Note, however, that this recommendation cannot be universal, being necessarily limited to ligand fields similar to those studied here. For instance, the hybrid functionals might not be optimal to describe coordination of an extra ligand to Co(acac)₂; this issue would require further studies. As already evident from many examples,^{11,15,16} DFT performance for spin-state energetics shows to be variable and capricious.

We also focused on the crystal structure of monomeric bis(acetylacetonate) cobalt(II) from ref 5 (containing square-planar molecules) in view of its putative contradiction with our calculations. Therefore, we estimated the energy of the intermolecular interactions in the crystal structure at MP2 and CC2 levels using dimer and trimer models. We found that the favorable interaction “felt” by a square-planar monomer might be strong enough (≥ 10 kcal/mol) to compensate for its intrinsically higher energy. This result supports the original hypothesis given in ref 6 at quantitative level and could explain the apparent discrepancy between theory (CASPT2, hybrid DFT) and the crystal structure.⁵ According to the relative spin state energetics presented here, most probably the high-spin state is “frozen” in the crystal structure.

It should be stressed here that BP86 or PBE results, predicting a planar conformation for an isolated Co(acac)₂ molecule, could be naively treated as “confirmed” in view of the crystal structure from ref 5. In fact, the optimal conformation of a single molecule is nonplanar, but the crystal structure is dominated by strong π -stacking interactions. Nota bene, BP86 and PBE are not able to properly describe these interactions. This is a methodological warning that the possibility of strong intermolecular interactions must be accounted for when judging the accuracy of quantum chemical methods on the basis of crystal structures.

Acknowledgment. We are thankful to Dr. Artur Michalak (Jagiellonian University) for focusing our attention on methodological problems with cobalt(II) bis(acetylacetonate). We also acknowledge Prof. Zbigniew Sojka and Prof. Piotr Petelenz (Jagiellonian University) for interesting discussions and Prof. Kristine Pierloot (University of Leuven) for valuable private communication. Special thanks to her Ph.D. student, Steven Vancoillie, for constructive remarks about the manuscript. This work was partially supported by computational grants from the Academic Computer Center CYFRONET AGH (Grant Nos.: MNiSW/SGI3700/UJ/133/2006, MNiSW/SGI4700/UJ/085/2007, and MNiSW/IBM_BC_HS21/UJ/085/2007). Molecular structures in Figures 1 and 3 were prepared with the XYZViewer program, courtesy of its author, Sven de Marothy (Stockholm University, 2003–2004).

Supporting Information Available: The PBE0/A structures, the contour plots of the orbitals discussed in section 2, and the estimation of solvent effects and relative zero-point vibrational energies. This material is available free of charge via the Internet at <http://pubs.acs.org>.

References

- (1) Kaneyoshi, H.; Matyjaszewski, K. *Macromolecules* **2005**, *38*, 8163–8169.
- (2) Cotton, F. A.; Holm, R. H. *J. Am. Chem. Soc.* **1960**, *82*, 2979–2983.
- (3) Cotton, F. A.; Soderberg, R. H. *Inorg. Chem.* **1964**, *3*, 1–5.
- (4) Cotton, F. A.; Elder, R. C. *Inorg. Chem.* **1965**, *4*, 1145–1151.
- (5) Burgess, J.; Fawcett, J.; Russell, D. H.; Gilani, S. R. *Acta Crystallogr.* **2000**, *C56*, 649–650.
- (6) Maria, S.; Kaneyoshi, H.; Matyjaszewski, K.; Poli, R. *Chem.—Eur. J.* **2007**, *13*, 2480–2492.
- (7) Srebro, M.; Pietrzyk, P.; Michalak, A.; Sojka, Z. To be submitted for publication.
- (8) Nindakova, L.; Shainyan, B.; Saraev, V.; Chipanina, N.; Umanetz, V. *J. Mol. Catal. A: Chem.* **2005**, *235*, 161–172.
- (9) Debuigne, A.; Champouret, Y.; Jérôme, R.; Poli, R.; Detrembleur, C. *Chem.—Eur. J.* **2008**, *14*, 4046–4059.
- (10) Debuigne, A.; Michaux, C.; Jérôme, C.; Jérôme, R.; Poli, R.; Detrembleur, C. *Chem.—Eur. J.* **2008**, *14*, 7623–7637.
- (11) Harvey, J. N. *Annu. Rep. Prog. Chem., Sect. C: Phys. Chem.* **2006**, *102*, 203–226.
- (12) Roos, B. O.; Taylor, P. R.; Siegbahn, P. E. M. *Chem. Phys.* **1980**, *48*, 157–173.
- (13) Andersson, K.; Malmqvist, P.-Å.; Roos, B. O. *J. Chem. Phys.* **1991**, *96*, 1218–1226.
- (14) Pierloot, K. *Mol. Phys.* **2003**, *101*, 2083–2094.
- (15) Pierloot, K.; Vancoillie, S. *J. Chem. Phys.* **2006**, *125*, 124303.
- (16) Pierloot, K.; Vancoillie, S. *J. Chem. Phys.* **2008**, *128*, 034104.
- (17) Ahlrichs, R.; Horn, H.; Schaefer, A.; Treutler, O.; Haeser, M.; Baer, M.; Boecker, S.; Deglmann, P.; Furche, F. *Turbomole*, version 5.9; Universität Karlsruhe: Karlsruhe, Germany.
- (18) Frisch, M. J.; Trucks, G. W.; Schlegel, H. B.; Scuseria, G. E.; Robb, M. A.; Cheeseman, J. R.; Montgomery, J. A., Jr.; Vreven, T.; Kudin, K. N.; Burant, J. C.; Millam, J. M.; Iyengar, S. S.; Tomasi, J.; Barone, V.; Mennucci, B.; Cossi, M.; Scalmani, G.; Rega, N.; Petersson, G. A.; Nakatsuji, H.; Hada, M.; Ehara, M.; Toyota, K.; Fukuda, R.; Hasegawa, J.; Ishida, M.; Nakajima, T.; Honda, Y.; Kitao, O.; Nakai, H.; Klene, M.; Li, X.; Knox, J. E.; Hratchian, H. P.; Cross, J. B.; Bakken, V.; Adamo, C.; Jaramillo, J.; Gomperts, R.; Stratmann, R. E.; Yazyev, O.; Austin, A. J.; Cammi, R.; Pomelli, C.; Ochterski, J. W.; Ayala, P. Y.; Morokuma, K.; Voth, G. A.; Salvador, P.; Dannenberg, J. J.; Zakrzewski, V. G.; Dapprich, S.; Daniels, A. D.; Strain, M. C.; Farkas, O.; Malick, D. K.; Rabuck, A. D.; Raghavachari, K.; Foresman, J. B.; Ortiz, J. V.; Cui, Q.; Baboul, A. G.; Clifford, S.; Cioslowski, J.; Stefanov, B. B.; Liu, G.; Liashenko, A.; Piskorz, P.; Komaromi, I.; Martin, R. L.; Fox, D. J.; Keith, T.; Al-Laham, M. A.; Peng, C. Y.; Nanayakkara, A.; Challacombe, M.; Gill, P. M. W.; Johnson, B.; Chen, W.; Wong, M. W.; Gonzalez, C.; Pople, J. A. *Gaussian 03*, revision C.02; Gaussian, Inc.: Wallingford, CT, 2004.
- (19) Dolg, M.; Wedig, U.; Stoll, H.; Preuss, H. *J. Chem. Phys.* **1987**, *86*, 866–872.
- (20) Hehre, W.; Ditchfield, R.; Pople, J. *J. Chem. Phys.* **1972**, *56*, 2257–2261.
- (21) Francl, M.; Petro, W.; Hehre, W.; Binkley, J.; Gordon, M.; DeFrees, D.; Pople, J. *J. Chem. Phys.* **1982**, *77*, 3654–3665.

- (22) Weigend, F.; Furche, F.; Ahlrichs, R. *J. Chem. Phys.* **2003**, *119*, 12753–12762.
- (23) Weigend, F.; Häser, M.; Patzelt, H.; Ahlrichs, R. *Chem. Phys. Lett.* **1998**, *294*, 143–152.
- (24) Becke, A. D. *Phys. Rev. A* **1988**, *38*, 3098–3100.
- (25) Perdew, J. P. *Phys. Rev. B* **1986**, *33*, 8822–8824.
- (26) Perdew, J. P.; Burke, K.; Ernzerhof, M. *Phys. Rev. Lett.* **1996**, *77*, 3865–3868.
- (27) Handy, N. C.; Cohen, A. J. *Mol. Phys.* **2001**, *99*, 403–412.
- (28) Lee, C.; Yang, W.; Parr, R. G. *Phys. Rev. B* **1988**, *37*, 785–789.
- (29) Tao, J.; Perdew, J. P.; Staroverov, V. N.; Scuseria, G. E. *Phys. Rev. Lett.* **2003**, *91*, 146401–146404.
- (30) Perdew, J. P.; Ernzerhof, M.; Burke, K. *J. Chem. Phys.* **1996**, *105*, 9982–9985.
- (31) Becke, A. D. *J. Chem. Phys.* **1993**, *98*, 5648–5652.
- (32) Staroverov, V. N.; Scuseria, G. E.; Tao, J.; Perdew, J. P. *J. Chem. Phys.* **2003**, *119*, 12129–12137.
- (33) Klamt, A. *J. Phys. Chem.* **1995**, *99*, 2224–2235.
- (34) Andersson, K.; Barysz, M.; Bernhardsson, A.; Blomberg, M.; Cooper, D.; Fülscher, M.; de Graaf, C.; Hess, B.; Karlström, G.; Lindh, R.; Malmqvist, P.-Å.; Nakajima, T.; Neogrady, P.; Olsen, J.; Roos, B.; Schimmelpfennig, B.; Schütz, M.; Seijo, L.; Serrano-Andrés, P. E. M.; Siegbahn, J. S.; Thorsteinsson, T.; Veryazov, V.; Widmark, P.-O. MOLCAS, version 6.4, Lund University: Lund, Sweden, 2006.
- (35) Karlström, G.; Lindh, R.; Malmqvist, P.-Å.; Roos, B.; Ryde, U.; Veryazov, V.; Widmark, P.-O.; Cossi, M.; Schimmelpfennig, B.; Neogrady, P.; Seijo, L. *Comput. Mater. Sci.* **2003**, *28*, 222–239.
- (36) Ghigo, G.; Roos, B.; Malmqvist, P.-Å. *Chem. Phys. Lett.* **2004**, *396*, 142–149.
- (37) Pierloot, K.; Dumez, B.; Widmark, P.-O.; Roos, B. *Theor. Chim. Acta* **1995**, *90*, 87–114.
- (38) Roos, B. O.; Lindh, R.; Malmqvist, P.-Å.; Veryazov, V.; Widmark, P.-O. *J. Phys. Chem. A* **2005**, *109*, 6575–6579.
- (39) Reiher, M.; Wolf, A. *J. Chem. Phys.* **2004**, *121*, 10945–10956.
- (40) Boys, S. F.; Bernardi, F. *Mol. Phys.* **1970**, *19*, 553–566.
- (41) Christiansen, O.; Koch, H.; Jorgensen, P. *Chem. Phys. Lett.* **1995**, *243*, 409–418.
- (42) Conradie, J.; Quarless, D.; Hsu, H.-F.; Harrop, T.; Lippard, S.; Koch, S.; Ghosh, A. *J. Am. Chem. Soc.* **2007**, *129*, 10446–10456.
- (43) Neese, F. *J. Biol. Inorg. Chem.* **2006**, *11*, 702–711.
- (44) Güell, M.; Luis, J. M.; Solà, M.; Swart, M. *J. Phys. Chem. A* **2008**, *112*, 6384–6391.
- (45) Reiher, M.; Salomon, O.; Hess, B. A. *Theor. Chem. Acc.* **2001**, *107*, 48–55.
- (46) Fouqueau, A.; Mer, S.; Casida, M. E. *J. Chem. Phys.* **2004**, *120*, 9473–9486.
- (47) National Institute of Science and Technology (NIST) Atomic Spectra Database. http://www.physics.nist.gov/cgi-bin/AtData/main_asd (Accessed December 2008).
- (48) Jeziorski, B.; Moszynski, R.; Szalewicz, K. *Chem. Rev.* **1994**, *94*, 1887–1930.
- (49) Zhao, Y.; Truhlar, D. G. *Phys. Chem. Chem. Phys.* **2005**, *7*, 2701–2705.
- (50) Conradie, J.; Ghosh, A. *J. Phys. Chem. B* **2007**, *111*, 12621–12624.
- (51) Aquilante, F.; Malmqvist, P.-Å.; Pedersen, T. B.; Ghosh, A.; Roos, B. O. *J. Chem. Theory Comput.* **2008**, *4*, 694–702.

CT800571Y